

Motion Control and Simulation of a Towing Tank system in an Experimental Water Pool*

Min Xiao

College of Computer and Information Technology
China Three Gorges University
Yichang, 443002, China

Abstract

The underwater towed system is extensively used for various oceanic applications and military tasks etc., it is an important problem in the design and application of towed system to study its motion characteristics and control problems. It has very important meanings in the design and use of towed systematic to hold the law and characteristic of the systematic movement accurately. Trailer of towing tank is the basic equipment which is used for performance test of ship, and which role is to drag ship model or others for uniform motion in the tank, to measure the relevant performance parameters of ship after speed stable, to prediction and validation of the merits or inferiors of hull form design. As trailers uniform model accuracy directly affects the velocity and the accuracy of test results, which must be equipped with good speed control system which has high precision and immunity in order to ensure tow-speed precision movement. In this paper, through the establishment of a rigorous theoretical model, the object study is systematically analyzed and simulated by numerical simulation. The whole process of the design and simulation of the trailer movement control system is completed. The study of this paper lays the foundation for the development of successful underwater towing system for laboratory model test and offshore field prototype test.

Keywords: Towed system, resistance calculation, anti-skid analysis, process segment, speed control, position control

1. Introduction

An aquatic towing system is an effective method to carry scientific measuring equipment for aquatic search activities and military reconnaissance. In this study, a controllable aquatic towing system in a test water pool that meets task requirements and is practical was designed and developed. Based on the simulation of the motion control of the aquatic towing system in a test water pool, the calculation of the driving power of the trailer for the test object and the design control strategy for the trailer system velocity and position were analyzed. The results meet the requirements of the motion parameters of the test object. To research the systematic hydrodynamic performance, to set up one comparatively perfect simulation system to simulate various kinds of movement and make use of simulation system to adjust the design project of the towed system, is of great advantage to design and research towed system, it can save a large amount of time and fund, and avoid the enormous losses of manpower and material resources.

2. System overview

The primary function of a towing-test water pool is to accommodate the towed paths of a test object in different positions while measuring various motion parameters of the test object, such as resistance coefficient and position derivative. A sketch of the towing water pool is shown in Fig.1.

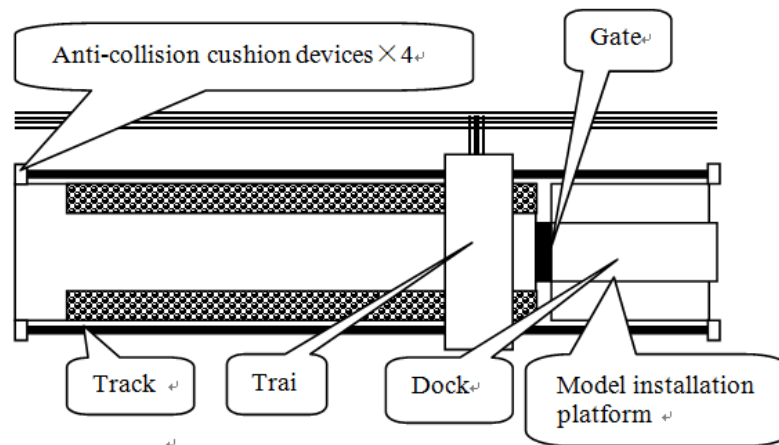


Fig.1 Components and layout of the non-standard equipment in the towing water pool

The towing test area consists primarily of a $170m$ (length, including dock) $\times 7m$ (water surface width) $\times 6m$ (water depth) towing water pool and model installation dock. The trailer, which is installed across the pool on tracks at both sides of the water pool, drags the test object and acts as a test platform. A trailer motor drives the motion of the wheel along the tracks. The trailer is $8m$ long and $7.5m$ wide. The trailer motion is as follows. The trailer control system starts up and accelerates the trailer. When the trailer reaches the specified test velocity (the maximum velocity is $7m/s$), acceleration stops and the trailer moves at a constant velocity. After a period of constant velocity, the test system is started. When the test is completed, the control system is activated to decelerate the trailer and stop the motion. The trailer is returned to dock, at which time the test is completed. The trailer, with a dead weight of $20t$ (excluding the test object), is supported by 4 wheels, bearing the weight equally. The trailer is driven by the 4 wheels synchronously. Each wheel is driven by a servo motor. The wheels are fabricated with hard steel; the track is fabricated with steel. The friction between the wheel and the track is modeled as steel-steel friction. The wheel diameter is $\phi 600mm$. The wheel axis and the motor axis are connected via a straight gear decelerator with a deceleration ratio equal to 8 and a motor rotation rate equal to $1500rpm$. An aircraft model, the test object, is installed at the bottom of the trailer via a connector (no longer than $2m$), completely submerged in water and moving in tandem with the trailer.

The following are the relevant parameters: the test length is $7m$; the test apparatus weight is $1.5t$; the drainage capability is $1.5t$; the underwater weight is 0 ; the underwater resistance is $F_{water} = A_x V^2$, where V is the trailer velocity; and the overall maximum resistance coefficient of the model is $A_x = 36$. The trailer has a truss-like structure; hence, windward resistance to motion should be taken into account. Windward resistance is calculated by $F_{wind} = C_x V^2$, where V is the trailer velocity, and the overall trailer windward resistance coefficient is $C_x = 15$. The following are the trailer motion parameters: the maximum velocity is $7m/s$; the maximum acceleration is $0.7m/s^2$; and the maximum deceleration is $-2.0m/s^2$ (hydraulic pressure track brake deceleration).

3. Slip and power torque calculation

Based on the conditions provided by the system, the maximum motor power and the maximum torque during trailer motion are calculated. During motion, dynamic underwater resistance and windward resistance should be considered. The specified test velocity, acceleration and deceleration should be reached, and wheel slip should not occur. Slip is related to two factors: The slip friction between the track and the wheel is related to the materials of both the wheel and the track, as well as to environmental factors, such as humidity, grease pollution and corrosion level. The tractive force is related to the motor power. The motor has limited power, and its acceleration and deceleration properties are also fixed. The maximum value of the tractive force is limited by the wheel maximum adhesive force, i.e., the maximum static friction. The occurrence of slip depends on whether the motion resistance is greater than the maximum adhesive force (maximum static friction) determined by the wheel pressure.

During motion, the trailer is affected by three different forces: the tractive force F , which results in trailer acceleration; the overall trailer pressure on the track F_n ; the trailer is a truss-like structure, whose windward resistance is $F_{wind} = C_x V^2$, underwater resistance is $F_{water} = A_x V^2$, and friction is $F_{friction}$. A simple model of the overall motion of the trailer from stress is shown in Fig. 2.

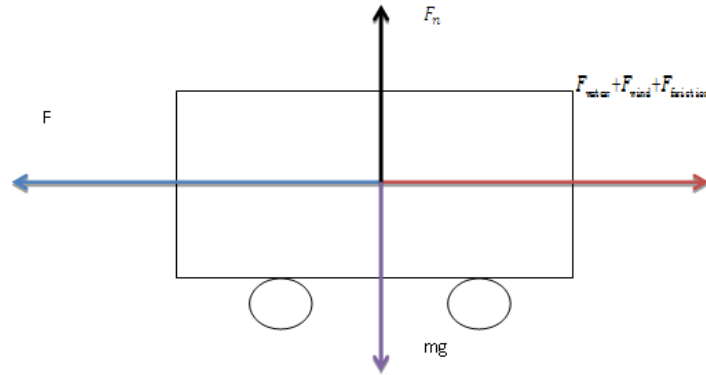


Fig. 2 Simplified diagram for overall trailer motion stress model During trailer acceleration, the tractive force $F_{acceleration}$ is as follows:

$$F_{acceleration} = F_{water} + F_{wind} + F_{friction} + ma \quad (1)$$

When the trailer is moving at a constant velocity, the tractive force $F_{constant}$ is as follows:

$$F_{constant} = F_{water} + F_{wind} + F_{friction} \quad (2)$$

When the trailer is decelerating, the brake force $F_{deceleration}$ is as follows:

$$F_{deceleration} = F_{water} + F_{wind} + F_{friction} - ma \quad (3)$$

In the above formulae, F_{water} is the underwater resistance, F_{wind} is the air resistance, $F_{friction}$ is the rolling friction, m is the mass, and a is the acceleration. The rolling friction $F_{friction}$ is normally measured using the resistance moment, a quantity determined by the properties, the surface shape and the weight of the rolling object. Rolling friction is a moment that hinders rolling. When an object rolls on a coarse plane, if no kinetic force or kinetic moment is applied, its motion will gradually decrease until it stops. During this process, the rolling object is affected by gravity and elasticity; the contact point is also affected by static friction.

Existing parameters are fully utilized to obtain a more accurate calculation. The wheel diameter is $\phi 600mm$, the wheel axis and the motor axis are connected via a straight gear decelerator, whose deceleration ratio is 8 and motor rotation rate is $1500rpm$. The overall trailer pressure on the track is F_n , k is the rolling friction coefficient, M is the moment, and R is the wheel radius. Based on the following relation:

$$M = k \cdot F_n = F_{rolling} \cdot R$$

and then $F_{rolling} = k \cdot F_n / R$

Based on the known test conditions, $R = 0.3m$ and $F_n = 20000 \times 9.8 = 196000N$. The rolling friction coefficient for steel-steel is set to $k = 0.005$, then the rolling friction $F_{friction}$ is as follows:

$$F_{rolling} = (0.005 \times 196000) / 0.3N = 3266.67N$$

If slip friction is not negligible, the friction coefficient can be adjusted properly to account for slip.

During the acceleration, the rolling wheel has a temporary change from slip to rolling. If system slip is not allowed, then the relation is as follows:

$$F_{wind} + F_{water} + F_{slip} \leq F \leq \mu mg + F_{wind} + F_{water} + F_{slip} \quad (4)$$

During the acceleration of the trailer, if slip is not allowed, then the force on the trailer is as follows:

$$F - (F_{wind} + F_{water} + F_{slip}) = ma \leq \mu mg \text{ and } a \leq \mu g$$

It is assumed that the track and the wheel are not corroded and are clean and dry; the steel-steel slip friction coefficient is calculated via $\mu = 0.15$. Therefore, the maximum acceleration during the acceleration is as follows:

$$\text{When } a_1 = \mu g = 0.15 \times 9.8 = 1.47 \text{ m/s}^2, \mu = 0.15$$

$$\text{When } a_1 = \mu g = 0.1 \times 9.8 = 0.98 \text{ m/s}^2, \mu = 0.1$$

Hence, when the maximum acceleration is 0.7 m/s^2 , trailer slip will not occur.

During constant velocity, there is $F_{\text{constant}} = F_{\text{wind}} + F_{\text{water}} + F_{\text{slip}}$, so slip will not occur.

During deceleration, there are occurrences of slip with a brake force and without a brake force; however, to prevent system slip, the brake force F' should satisfy the following:

$$0 < F' + F_{\text{wind}} + F_{\text{water}} + F_{\text{slip}} = ma \leq \mu mg \text{ and: } a \leq \mu g$$

Therefore, under the aforementioned parameters, the maximum theoretical deceleration range is as follows:

$$a_1 = \mu g = 0.15 \times 9.8 = 1.47 \text{ m/s}^2$$

The data showed that based on the control strategy requirement, within the system required range of maximum acceleration 0.7 m/s^2 and maximum deceleration of 2.0 m/s^2 , system slip will not occur.

Because the deceleration process uses a hydraulic pressure track brake deceleration, the system brake force is 0. To prevent system slip, the system resistance should be less than the maximum system static friction, i.e., the system slip friction, as follows:

$$0 < F_{\text{wind}} + F_{\text{water}} + F_{\text{slip}} \leq \mu mg$$

During system deceleration, if there is no slip, the resultant force is as follows:

$$ma = F_{\text{wind}} + F_{\text{water}} + F_{\text{slip}} \leq \mu mg \text{ thus: } a \leq \mu g$$

Therefore, under the aforementioned parameters, the maximum theoretical deceleration range during deceleration is as follows:

$$a_1 = \mu g = 0.15 \times 9.8 = 1.47 \text{ m/s}^2$$

Based on the system requirements and the above analysis, the towing system motion plan is as follows. During the acceleration phase, the system accelerates at a constant rate $a_1 = 0.7 \text{ m/s}^2$. When the maximum velocity V_{max} is reached, the velocity of the trailer is held constant for 12 s . The trailer then decelerates at a constant rate $a_2 = 1.47 \text{ m/s}^2$. This relation is described as follows:

$$\begin{cases} \frac{1}{2} a_1 t_1^2 + 12 V_{\text{max}} + \frac{1}{2} a_2 t_2^2 = 120 \\ V_{\text{max}} = a_1 t_1 = a_2 t_2 \end{cases}$$

Combining the above two formulae with the parameters yields the following:

$$\begin{cases} t_1 = 9.1339 \text{ (s)} \\ t_2 = 4.3495 \text{ (s)} \\ V_{\text{max}} = 6.3937 \text{ (m/s)} \end{cases}$$

In summary, the system motion strategy is as follows. During acceleration, the trailer accelerates at a constant rate of 0.7 m/s^2 for 9.1339 s . After reaching a maximum velocity of 6.3937 m/s , the trailer continues at a constant velocity for 12 s . The trailer then decelerates at a constant rate of 1.47 m/s^2 for 4.3495 s until the system motion stops. The stroke for the entire process is 119.8291 m .

According to the formula for motor power, $P = FV$, when F and v are maximum values, power P is also a maximum. For example, assume that velocity v is at its maximum value. As long as acceleration a is also at its maximum value, F is also at a maximum value. When $V_{\text{max}} = 7 \text{ m/s}$, there are two scenarios for acceleration:

$a_1 = 0.7 \text{ m/s}^2$ during trailer acceleration and $a_2 = 1.47 \text{ m/s}^2$ during deceleration. The data show that the tractive force F during trailer acceleration is greater than the tractive force F during deceleration. Therefore, when the trailer velocity is 6.3937 m/s and the acceleration is 0.7 m/s^2 , i.e., when the trailer accelerates from a maximum velocity of 0.7 m/s^2 to a maximum velocity of 6.3937 m/s , the tractive force F at this moment is the maximum F ; the motor power reaches its maximum value also.

$$F_{\max} = 51 \times 6.3937^2 + 20000 \times 0.7 + 3266.67 = 19351.51938419N$$

The maximum power is as follows:

$$P_{\max} = F_{\max} \cdot V_{\max} = 19351.51938419 \times 6.3937 = 123.7278KW$$

The maximum torque is the following:

$$T_{\max} = 9550 \cdot P_{\max} / n$$

where n is the motor rotation rate, $n = 1500rpm$.

Hence, the maximum torque is as follows:

$$T_{\max} = 9550 \cdot 123.7278 / 1500 = 787.7337NM$$

4. Accurate control of velocity and position at transition segments

- The process of start, acceleration, stabilization, deceleration and stop should be completed in the stroke range of $120m$; slip should not occur during acceleration and deceleration. Acceleration should not exceed $0.7m/s^2$; maximum deceleration should not exceed $2.0m/s^2$ (hydraulic pressure track brake deceleration); and the maximum velocity is $7m/s$. After accelerating to the maximum velocity, the trailer is stabilized for $1s$. Then, the trailer moves at a constant velocity for $10s$ to perform object testing. When the test is complete, the trailer continues at a constant velocity for $1s$. Next, the deceleration starts, continuing until the trailer stops.
- Velocity stability requirements: When the velocity is less than $1m/s$, the velocity fluctuations should be less than 0.3% . When the velocity is greater than or equal to $1m/s$, the velocity fluctuations should be less than 0.1% . Finally, the maximum velocity is $7m/s$. Based on requirements above, the strategy for the trailer motion is designed, which includes the motion stroke distribution at acceleration, the stabilization, the deceleration segment, the variable or constant acceleration and the deceleration strategy.
- When the motion stroke is greater than $10m$ and the average velocity is $3.5m/s$, the positioning accuracy should be $\leq 5mm$; When the motion stroke is less than $10m$ and the duration of the motion is less than 8 seconds, the positioning accuracy should be $\leq 5mm$; During the positioning and movement of the trailer, overshoot should not occur. Based on requirements above, the strategy for the trailer motion is designed, which includes the motion stroke distribution at acceleration, the stabilization, the deceleration segment, the variable or constant acceleration and the deceleration strategy. The system velocity and expected time goal are shown in Fig. 3.

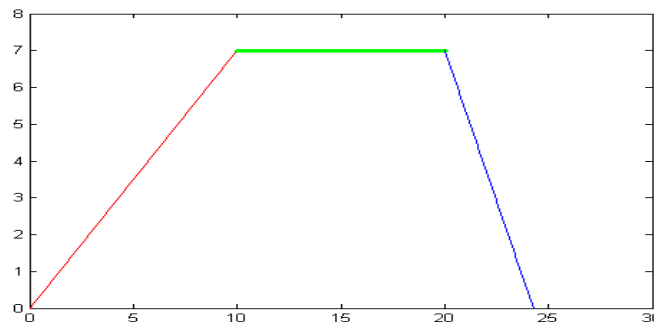


Fig. 3 Form of the expected velocity goal

The expected velocity of the trailer, shown in Fig. 3, in the acceleration, constant velocity and deceleration segments is linear. The acceleration segment and the deceleration segment can be controlled via the linear control rule. Power at a constant velocity segment is a constant. From an engineering perspective, to ensure stable and smooth transition of the system and eliminate overshoot during transition from the acceleration segment to the constant velocity segment and from the constant velocity segment to the deceleration segment, the problem becomes the adjustment of the transition segment control for the following target segments:

- Transition between the acceleration segment and the constant velocity segment.
- Transition between the constant velocity segment and the deceleration segment. Based on a high-reliability transition segment program control method verified in actual engineering, i.e., exponential program control, power P is reconstructed as a function of time t , which provides time-based output power independently to control tractive force and obtain expected slide block motion velocity. Slide block velocity control is

performed via the following control mode: $P \rightarrow F \rightarrow V$

The tractive force is controlled by controlling power and eventually to achieve the expected goal of controlling velocity. However, further analysis shows that $P(V), F(V)$ are both functions of V . Therefore, when conventional feedback control is applied, the situation shown in Fig. 4 will occur.

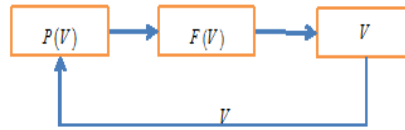


Fig. 4 Feedback diagram for velocity control rule

As velocity v is both a control variable and a control parameter, a closed-loop coupling state is formed, which will eventually become a control loop. Therefore, decoupling is required. Because motor control is essential to control motor output power, the parameterization of motor output power is redesigned. Analytic methods and dynamic decoupling methods are employed. When these methods are applied to program control of an aircraft transition segment, exponential program control is employed to reconstruct power P as a function of time t , which provides time-based output power independently to control tractive force and obtain expected slide block velocity.

The general expression for the program control rule for the relation between power and time is as follows:

$$P = f(t)$$

The formula for the velocity-time function during acceleration is as follows:

$$v_1 = a_1 t (0 \leq t \leq 9.1339)$$

The formula for the velocity-time function during the constant velocity period is as follows:

$$v_2 = 6.3937t (9.1339 < t \leq 21.1339)$$

The formula for the velocity-time function during deceleration is:

$$v_3 = 6.3937 - a_2(t - 21.1339) (21.1339 < t \leq 25.4834)$$

To ensure smooth and stable function transition in each segment, parameterization design for these functions in the form of time domain step function is as follows:

$$\begin{cases}
 P = 1.2373 \times 10^5 \frac{t}{9.1339} & t \leq 8.8 \\
 P = 1.2373 \times 10^5 \times e^{-\frac{(t-9.5)^2}{3.6^2}} & 8.8 < t \leq 9.5 \\
 P = 34216 & 9.5 < t \leq 20.5 \\
 P = 1.5376 \times 10^5 \times e^{-\frac{(t-20.5)^2}{3.58^2}} & 20.5 < t \leq 21.4 \\
 P = 1.5376 \times 10^5 \times \frac{1 - (t - 21.1339)}{4.3495} & 21.4 < t \leq 25.4834
 \end{cases}$$

This type of control rule requires no control variable feedback, has simple structure and is easy to implement in hardware. Simulation results are shown in Fig. 5-7.

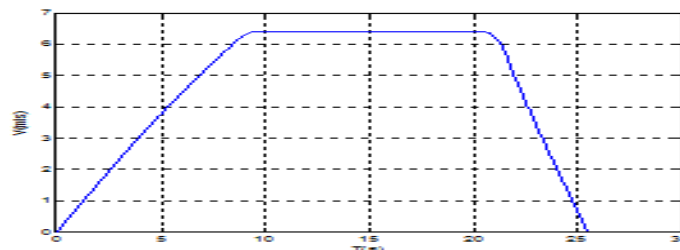


Fig. 5 Velocity control simulation result

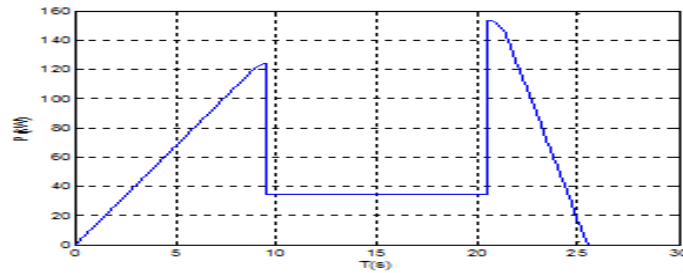


Fig. 6 Power output control simulation result

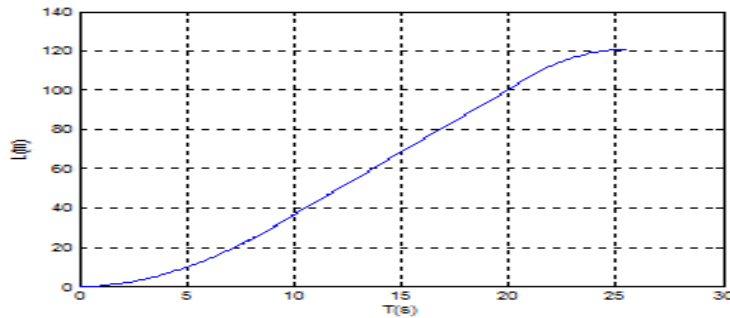


Fig. 7 Slide block stroke simulation result

The simulation results show that this control system can effectively control the slide block velocity and stroke; the velocity control meets the expected control goal; the final stroke is 120.7223 m, which matches the ideal state of 119.8288 m well. These results show the effectiveness of the control system. An accurate control model uses a segment function to approximate the expected goal; in each moment, it is acceptable as long as the difference between the motion distance simulation result and expected goal satisfies the required accuracy. In cases where more accurate control for the transition segment is required, a proportional integral derivative (PID) micro-adjustment capability can be added to the program control. The general formula for control is as follows:

$$P = f(t) + K\Delta V$$

Assume that $K = -500$.

Simulation results based on this control rule are shown in Figs. 8-10.

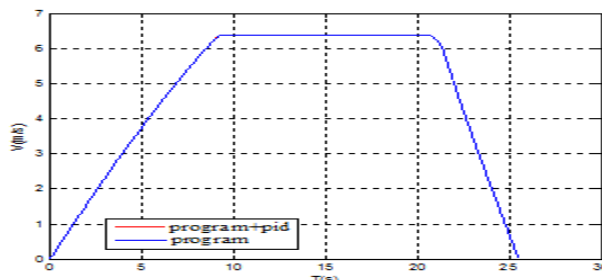


Fig. 8 Comparison of the simulation result of slide block stroke program control versus the result of program + PID adjustment

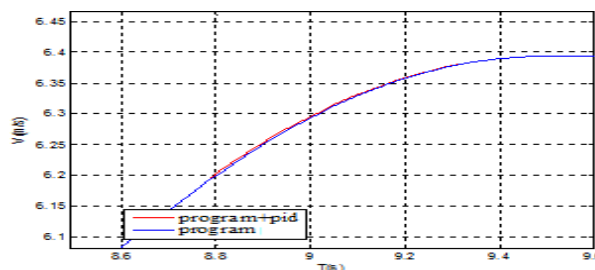


Fig. 9 Comparison of the simulation result of slide block velocity program control versus the result of program + PID adjustment

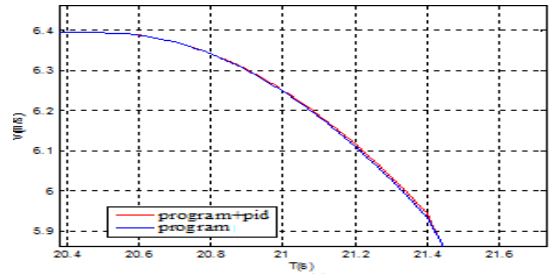


Fig. 10 Comparison of the simulation result of slide block velocity program control versus the result of program + PID adjustment

As shown in the above diagrams, based on this control rule, the transition segment can be smoothed further. Comparison shows that the result matches that of the original program control, while this control rule costs more to implement. Even though, based on the control rule, the transition segment can be smoothed further. The macroscopic effect matches that of the original program control. From a practical engineering perspective, this control rule has a higher implementation cost.

5. Process segment acceleration control and trailer position accuracy control

It is relatively difficult to accurately control the velocity in the form of trapezoid straight line required by the system via exponential velocity control. Acceleration control strategy is applied to improve control accuracy. In actual applications, it is more convenient to use an acceleration sensor for measurement to achieve more accurate control and to facilitate engineering implementation.

Control time sequence analysis shows that the control process is as follows:

$$P \rightarrow F \rightarrow a$$

The control goal is distance; however, the actual expected control goal is acceleration a , which is a phase function. Therefore, slide block control is actually the problem of how to obtain the expected acceleration in a different time domain, as shown in Fig. 11.

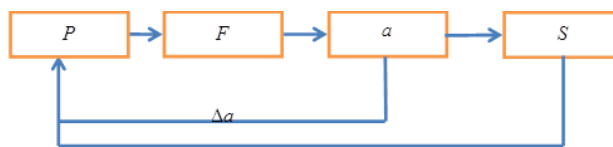


Fig. 11 Control feedback diagram here $F = K_1\Delta x_1 + K_2\Delta x_2$ Where K_1, K_2 are control coefficients and $\Delta x_1, \Delta x_2$ are offsets.

Based on the PID control goal, the expected objective function selection criteria is to choose a constant distance offset or a posture angle. The offset between the current goal and the expected goal is adjusted to ensure that the control object reaches the expected goal. Even though the final goal of the design object is displacement, the slide block motion is analysed: rising velocity (state I), stable velocity (state II) and declining velocity (state III). In the above three processes, the actual constraint acceleration of the slide block motion is related to the motion period under such acceleration. Therefore, conventional PID control is applied, and the control diagram is as shown in Fig. 11.

In Fig. 11,

$$\Delta a = \begin{cases} k(t) & a < a_0 \\ 0 & a = a_0 \end{cases}$$

When the acceleration of the control object is equal to the expected acceleration a_0 , control becomes ineffective and a cycle is formed as follows:

(1) When $a < a_0$, the control system is effective, and the slide block acceleration quickly approaches expected acceleration, and

(2) when $a = a_0$, the control system is ineffective, and the slide block keeps moving at control system's final output velocity.

Because of the above states, decoupling is required. As the motor control eventually is the control over the motor output power, parameterization of motor output power is redesigned.

The velocity-time function during acceleration is as follows:

$$v_1 = 0.7t(0 \leq t \leq 10)$$

The velocity-time function during constant velocity is as follows:

$$v_2 = 7(10 \leq t \leq 20)$$

The velocity-time function during deceleration is as follows:

$$v_3 = 7 - 1.6333(t - 20)(20 \leq t \leq 24.2857)$$

Expected form of system velocity-time goal is as shown in Fig. 12.

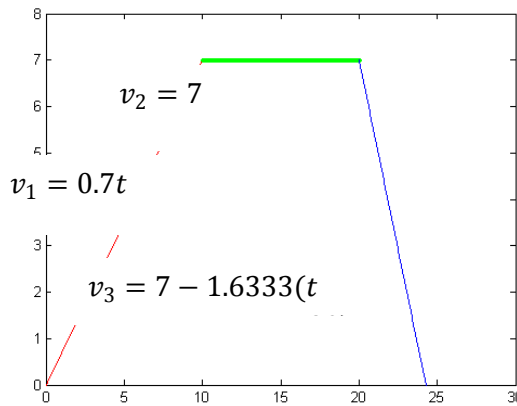


Fig. 12 Expected form of system velocity goal

Based on the transition segment program control method, exponential program control is employed to reconstruct power P as a function of phase time t . The slide block position is used as phase node feedback, which provides time-based output power independently to control tractive force and obtain expected slide block velocity. Simultaneously, the following control method is applied to ensure stable acceleration when the slides block acceleration changes:

$$P = \begin{cases} f_1(t) + K_1 \Delta a & S < S_1 \\ f_2(t) + K_2 \Delta a & S < S_2 \\ \dots & \\ f_n(t) + K_n \Delta a & S < S_n \end{cases}$$

Based on the above formula, $F = f(V), V = P/F, S = \dots$ are used to parameterize them in the form of a time domain step function as follows:

$$P = \begin{cases} P_1 \frac{t}{t_1} + (36V^2 + 15V^2 + 3266.67)V - 1000(a - a_1) & S \leq S_1 \\ (36V_0^2 + 15V_0^2 + 3266.67)V_0 & S_1 < S \leq S_2 \\ P_3 \left(1 - \frac{t - t_1 - t_2}{t_3} \right) + (36V^2 + 15V^2 + 3266.67)V - 1000(a - a_3) & S_2 < S \leq S_0 \end{cases}$$

where: P_1 is the maximum power in a rising velocity segment, $P_1 = ma_1V_0$; P_3 is the maximum power in a declining velocity segment, $P_3 = ma_3V_0$; V_0 is the expected stable velocity, $7m/s$; t_1, t_2, t_3 are the times of motion in the rising velocity segment, the stable velocity segment and the declining velocity segment, respectively; a_1, a_2, a_3 are accelerations in the rising velocity segment, the stable velocity segment and the declining velocity segment, respectively; and s_1, s_2, s_3, s_0 are displacement lengths in rising velocity segment, stable velocity segment, declining velocity segment and overall stroke. The applied control rule requires no end-to-end control variable feedback, has simple structure and is easy to implement in hardware. Under the above three velocity states, the slide block has 11 variables, which are $t_1, t_2, t_3, a_1, a_2, a_3, V_0, s_1, s_2, s_3, s_0$. However, the following are known variables:

$$V_0 = 7, a_1 = 0.7, a_2 = 0, t_2 = 12, S = 120 \quad (9)$$

The constraint relations among the variables are as follows:

$$t_1 = V_0 / a_1, s_1 = \frac{1}{2} a_1 t_1^2, s_2 = V_0 t_2, s_3 = S_0 - s_1 - s_2, a_3 = 2s_3 / t_3^2, a_3 = V_0 / t_3 \quad (10)$$

The formulae show that when five variables are obtained, the other seven variables can be calculated. Therefore, to change the control rule, only five variables must be changed. From among them, five variables need confirmation, i.e., V_0, a_1, s_0, t_2, a_2 .

Based on formula (9), expected displacement and expected velocity variation in the range of allowed displacement values are obtained.

When $V_0 = 7, a_1 = 0.7, a_2 = 0, t_2 = 12, S = 120$, the expected system velocity goal is obtained, as shown in Fig. 13.

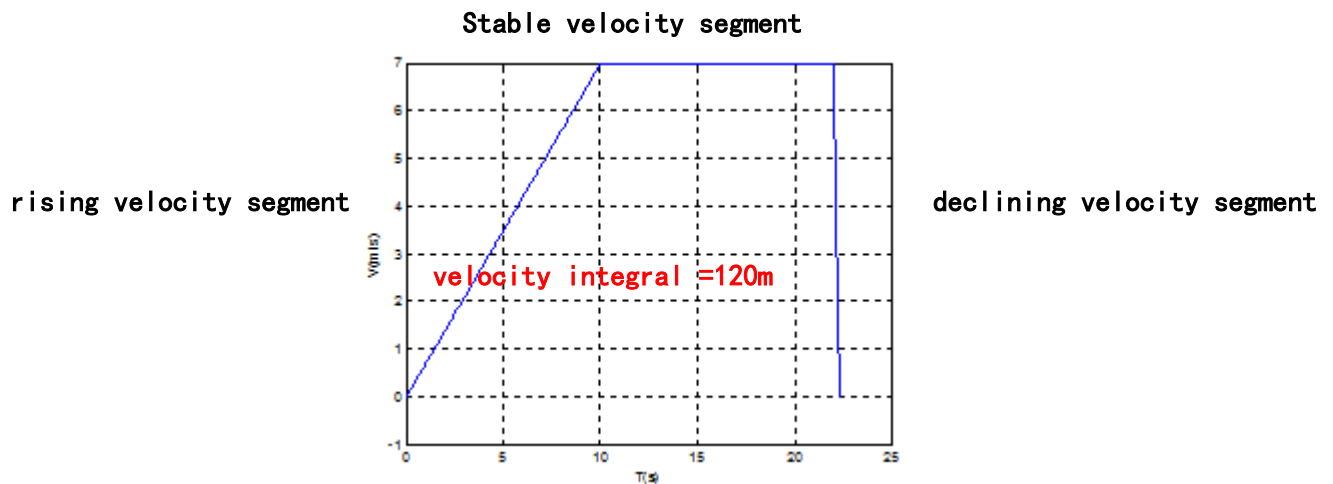


Fig. 13 Form of expected velocity goal

When $V_0 = 7, a_1 = 0.7, a_2 = 1.633, t_2 = 10, S = 120$, the expected system velocity goal is obtained, as shown in Fig. 14.

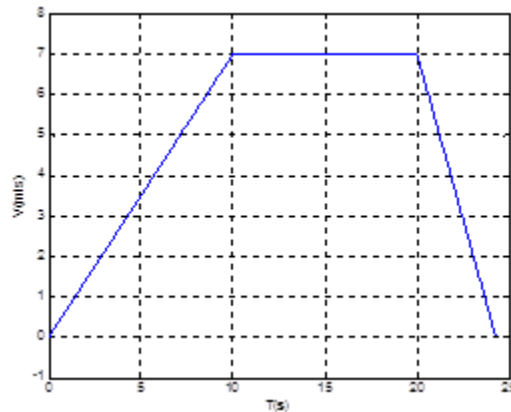


Fig. 14 Form of expected velocity goal

When $V_0 = 7, a_1 = 0.7, a_2 = 0, t_2 = 12, S = 120$, the simulation result is shown in Fig. 15-17.

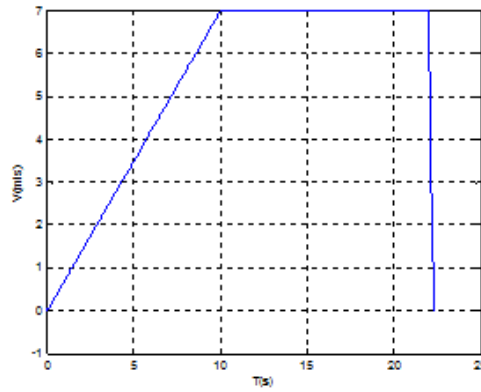


Fig. 15 Velocity control simulation result

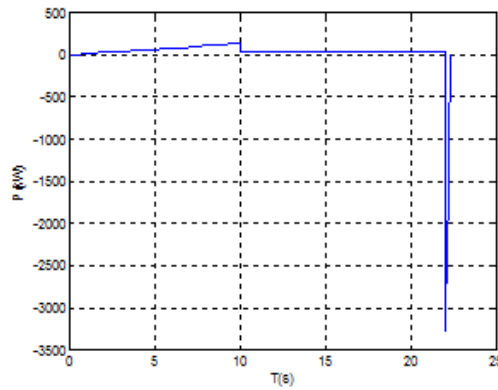


Fig. 16 Power output control simulation result at a constant velocity for $t = 12$ s

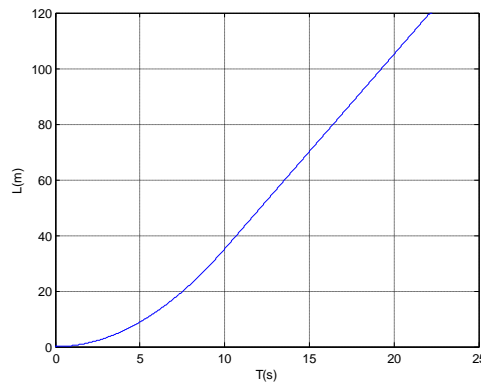


Fig. 17 Slide block stroke simulation result at a constant velocity for $t = 12$ s
 When $V_0 = 7, a_1 = 0.7, a_2 = 1.633, t_2 = 10, S = 120$, the simulation results are shown in Fig. 18-20.

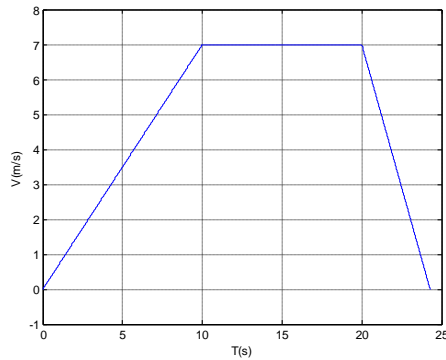


Fig. 18 Velocity control simulation result

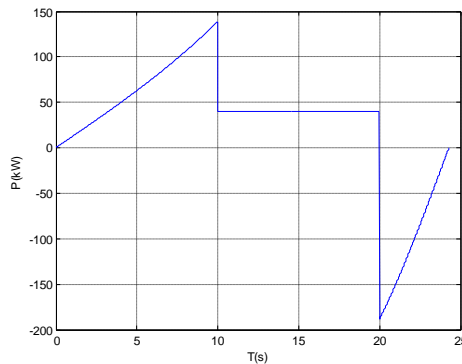


Fig. 19 Power output control simulation result at a constant velocity for t = 10 s

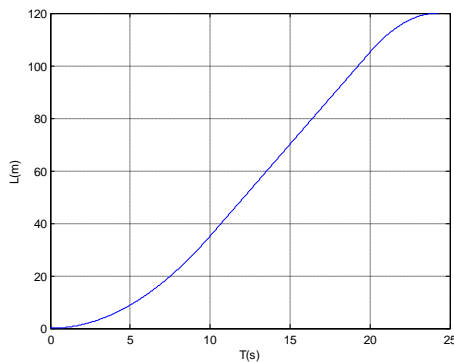


Fig. 20 Slide block stroke simulation result at a constant velocity for t = 10 s

The results of the simulation show that this control system can effectively control the slide block velocity and stroke; velocity control matches expected control goal; final stroke is 119.99 m, which matches the ideal state of 120 m well. This result shows the effectiveness of the control system operation. For a specific control system, how to perform theoretical qualitative analysis and quantitative calculation of dynamic performance and stable state accuracy and how to design proper correction device based on system performance requirement to ensure that system performance completely meets technological requirements are critical to guarantee accurate trailer position control.

To perform the design verification, let $\Delta L = L - L_0$. Based on the requirements, $\Delta L \leq 5mm$, where L_0 is the expected slide block displacement distance. The control accuracy model leverages the segment function to approximate the expected goal. At each step, the position is accepted if the difference between the motion distance simulation result and the expected goal meets the required accuracy. Simulation results are shown in Fig. 21-22.

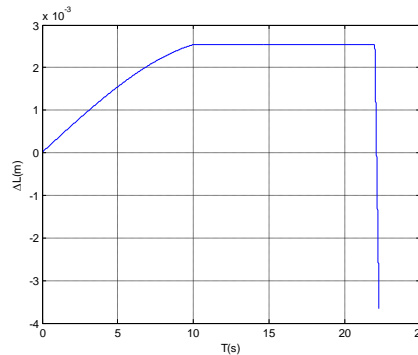


Fig. 21 Displacement control accuracy at a constant velocity for $t = 12$ s

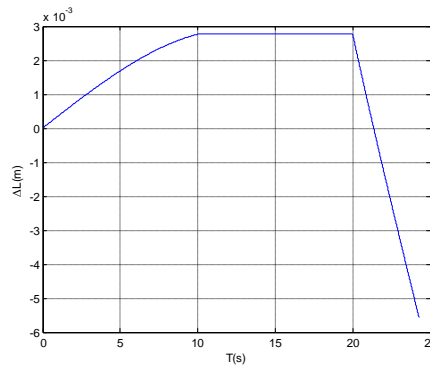


Fig. 22 Displacement control accuracy at a constant velocity for $t = 10$ s

The results show that the control accuracy in the entire domain satisfies the requirement of less than 5 mm error, indicating that the design plan is feasible.

6. Conclusions

Based on the requirement for parameters such as a towing water pool non-standard equipment component and overall layout, the simulation of the aquatic towing system motion control in a water pool is used to verify the design. In three states of motion, which include acceleration, constant velocity and deceleration, windward resistance and underwater resistance are included, friction and tractive forces are calculated, and slip is analysed. The maximum motor power and torque during trailer system motion are analysed and calculated. A trailer velocity accuracy control strategy is designed, which includes stroke distribution in acceleration, stable velocity and deceleration segments, variable or constant acceleration and deceleration strategies. Good acceleration and maximum velocity required by system design are achieved; accurate trailer position control strategy is designed and simulated. The transition segment is based on an exponential program decoupling control method; both velocity and acceleration control plans are provided. Control accuracies of the two control methods are simulated and compared. The results show that acceleration control is highly accurate and easy to implement and the hardware design is simple and requires no feedback adjustment. This method is universal and practical. Simulation has verified that the accuracy of this method meets the goal of the test requirement.

References

- Van S. H., Kim W. J., Kim D. H. Experimental Investigation of Local Flow around KRISO 3600TEU Container Ship Model in Towing Tank. *Journal of the Society of Naval Architects of Korea*, 37, 3, 1-10, 2000
- Bašić J., Degiuli N., Dejhalla R. Total resistance prediction of an intact and damaged tanker with flooded tanks in calm water. *Ocean Engineering*, 130, 83-91, 2017
- Marco A. D., Mancini S., Miranda S., et al. Experimental and numerical hydrodynamic analysis of a stepped planing hull. *Applied Ocean Research*, 64, 135-154, 2017
- Ali A., Maimun A., Ahmed Y. M., et al. Resistance Analysis of a Semi-SWATH Design Concept in Shallow Water. *Journal of Marine Science & Application*, 16, 2, 182-189, 2017

- Kiosidou E. D., Liarokapis D. E., Tzabiras G. D., et al. Experimental Investigation of Roughness Effect on Ship Resistance Using Flat Plate and Model Towing Tests. *Journal of Ship Research*, 2017
- A T R P S., Leong Z. Q., Ranmuthugala D., et al. Numerical investigation of the hydrodynamic interaction between two underwater bodies in relative motion. *Applied Ocean Research*, 51, 14-24, 2015
- Acanfora M., Luca F. D. An experimental investigation into the influence of the damage openings on ship response. *Applied Ocean Research*, 58, 62-70, 2016
- Wang F., Huang G. L, Deng D.H. The Design and Steady-State Simulation of Underwater Towed System. *Journal of Shanghai Jiaotong University*. 32, 4, 679-684, 2008